Numerical analysis of the thermal energy storage in cellular structures filled with phase-change material

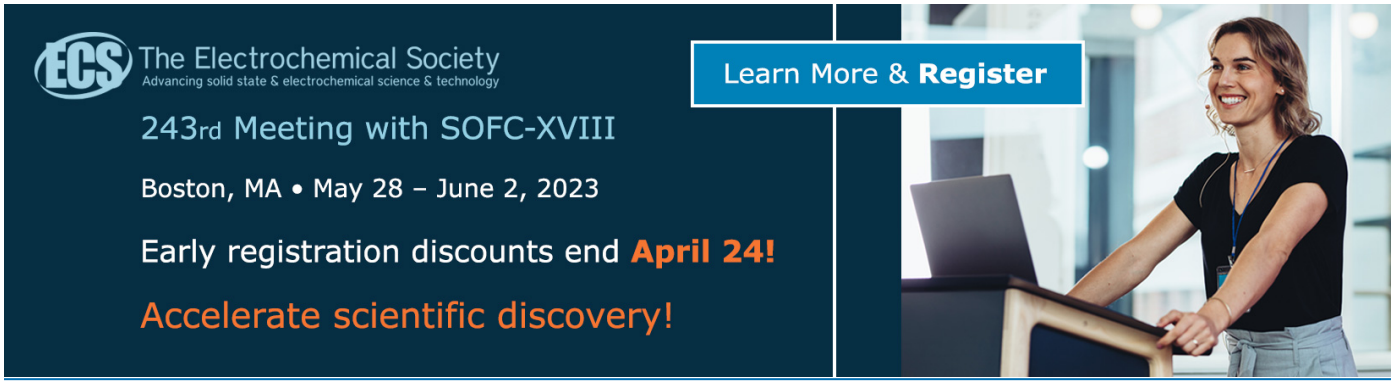

Numerical analysis of the thermal energy storage in cellular structures filled with phase-change material

Carlo Nonino[1], Andrea Diani[2], Luisa Rossetto[2]

[1]Dipartimento Politecnico di Ingegneria e Architettura, Università degli Studi di Udine, Via delle Scienze 206, 33100, Udine, Italy
[2]Dipartimento di Ingegneria Industriale, Università degli Studi di Padova, via Venezia 1, 35131 Padova, Italy

carlo.nonino@uniud.it

Abstract. This paper reports the results of a numerical study on the thermal performance of metal cellular structures that can be obtained by additive manufacturing (selective laser melting) when they are impregnated with phase change material (PCM) for possible applications in electronic cooling. Two body-centered cubic (BCC) periodic structures with cell sizes of 5 mm and 10 mm and a porosity of 87%, made of two solid materials (aluminum alloy and copper), and two paraffins with characteristic melting temperatures of 55 and 64 °C were considered. The numerical simulations are carried out using the commercial code ANSYS Fluent and are based on a previously validated purely conductive heat transfer model. The computational domains include just small repetitive portions of the considered composite structures, thus allowing substantial savings of computational time. Computed results show that, with both paraffins, the copper made finer BCC structure (5 mm) yields the best thermal performances, i.e, the shortest PCM melting time and the highest rate of thermal energy storage during transients.

1. Introduction

The ongoing green energy transition not only requires the adoption of suitable thermal energy storage techniques when energy supply and demand do not match, but also demands a more efficient use of energy. A phase change material (PCM) can serve the purpose in many cases, with applications ranging from electronics and battery cooling to manufacturing of solar collectors and passive building elements, just to mention a few. The variety of PCMs is rather broad and includes both inorganic and organic materials. Among the latter, paraffin waxes play an important role because they exhibit some very favorable characteristics such as a rather high latent heat, complemented with chemical stability and non-toxicity. All this makes them particularly suitable for electronic cooling [1,2], particularly in the cases of transient or intermittent applications [3–6]. However, paraffin waxes are also plagued by a low thermal conductivity, which makes the melting-solidification cycles inefficient. Therefore, several thermal conductivity enhancers like metal foams and fins have been proposed to increase the thermal performance of PCM based thermal energy storage systems [7–9]. The use of conductive fillers (e.g., carbon-based nanostructures or metal oxide nanoparticles) as thermal conductivity enhancers represents another viable solution [10].

Additive manufacturing (AM) technology can also be exploited to obtain 3D-printed metal cellular structures that can be used as an alternative to metal foams to increase the effective thermal conductivity of paraffin waxes. However, only few studies are available in the literature on the thermal behavior of PCM-impregnated structures obtained by AM [11–13]. Since the possibility of having a reliable estimate

of the performance of such composite structures is crucial for practical applications, in the attempt to fill, at least partially, a gap of knowledge, in this paper a numerical analysis is carried out on the thermal performance of body-centered cubic (BCC) periodic structures that can be obtained by AM (selective laser melting). Reference is made to a porosity of 87%, two cell sizes, two paraffins waxes and two different solid materials for the metal matrix. A simplified numerical model, previously validated through comparison with experimental data [14], is employed for the numerical simulations of thermal transients in the PCM-impregnated structures.

2. Statement of the problem

The periodic structures considered in this work consist of an assembly of body-centered cubic (BCC) cells. A BCC cell can ideally be obtained as the intersection of nine spheres, eight of them with their centers at the vertices of a cube and one with the center in the middle of the same cube. It must be pointed out that, since the AM technology cannot deal with very thin edges, the cells that can actually be 3D-printed are slightly modified BCC cells as that depicted in figure 1(a). The numerical analysis was carried out with reference to two cell sizes (5 mm and 10 mm) forming a periodic structure with a porosity of 87% and a total thickness of 20 mm, thus including two and four layers of cells, respectively. The demonstrative samples shown in figures 1(b) and (1c) were fabricated by selective laser melting. In the present study, two solid materials were assumed for the metal matrix, namely, an aluminum alloy (AlSi10Mg) and copper. Their relevant thermophysical properties are reported in table 1. In the following, based on the cell size and the material, the structures are identified as: BCC5-Al, BCC5-Cu, BCC10-Al, BCC10-Cu, with the obvious meaning of the acronyms.

Table 1. Thermophysical properties of solid materials.

Property	**AlSi10Mg**	**Cu**	**Units**
Specific heat capacity	871	381	[J kg^{-1} K^{-1}]
Thermal conductivity	175	387.6	[W m^{-1} K^{-1}]
Density	2719	8978	[kg m^{-3}]

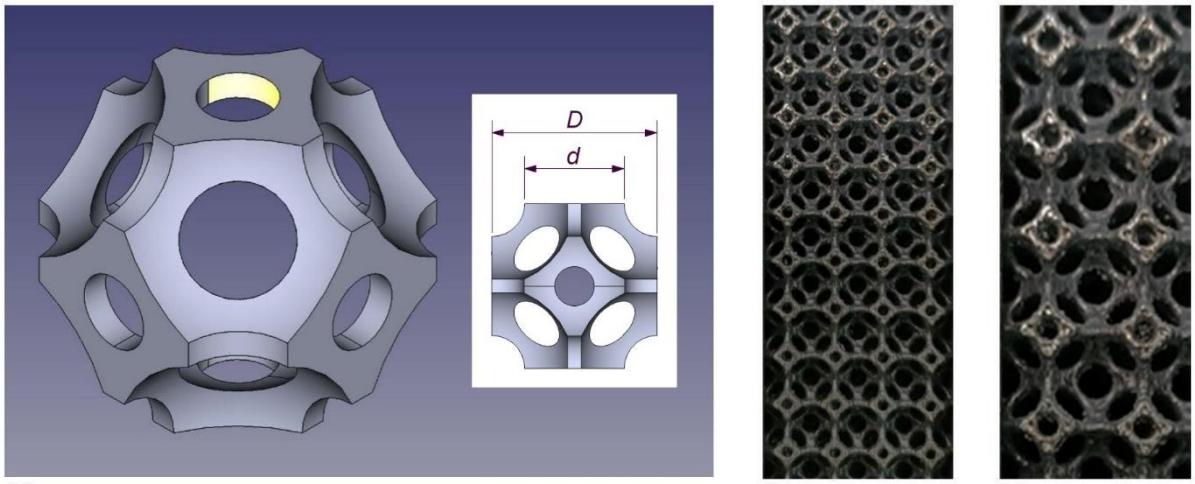

Figure 1. BCC cells: (a) schematic representation of a modified BCC cell; demonstrative samples of 3D-printed 20 mm thick BCC periodic structures with cells of main dimensions (b) D = 5 mm and d = 3 mm and (c) D = 10 mm and d = 6 mm.

Table 2. Thermophysical properties of paraffins [15].

Property	**RT55**	**RT64HC**	**Units**
Melting temperature range	51÷57	63÷65	[°C]
Heat storage capacity[a]	170	250	[kJ kg^{-1}]
Specific heat capacity	2	2	[kJ kg^{-1} K^{-1}]
Solid density[b]	880	880	[kg m^{-3}]
Liquid density[c]	770	780	[kg m^{-3}]
Thermal conductivity	0.2	0.2	[W m^{-1} K^{-1}]
Volume expansion	14	11	[%]

[a] Combination of latent and sensible heat in a temperature range of 48 and 63°C for RT55, of 57 and 72°C for RT64HC
[b] Evaluated at 15 °C for RT55, at 20 °C for RT64HC
[c] Evaluated at 80 °C

The thermal behavior of the PCM-impregnated metal matrices was studied with reference to two paraffin waxes with characteristic melting temperatures of 55°C and 64°C, manufactured by Rubitherm Technologies GmBH and identified as RT55 and RT64HC, respectively [15]. The thermophysical properties of the paraffines are reported in table 2. To assess the thermal performance of the composite structures in temperature intervals that included the melting temperature range of each wax, transient numerical simulations were carried out where the initial temperature was a few degrees below the initial melting temperature of the PCM and one of the sides was set at a temperature a few degrees higher than the final melting temperature, while all the other sides were assumed adiabatic. Thus, initial temperatures of 49°C and 57°C, were assumed for the RT55 and RT64HC waxes, respectively, while the corresponding temperatures of the heated surfaces T_{heat} were set at 59°C and 67°C.

3. Numerical model

Based on literature data [16] and on the results of previous experimental test [12,14], the effects of natural convection can be considered negligible in the conditions assumed for this analysis due to the suppression of the molten PCM motion by the metal matrix. Therefore, the numerical simulations were carried out adopting a purely conductive heat transfer model that was implemented using the finite volume commercial code ANSYS Fluent [17]. Consequently, it was not necessary to solve the Navier-Stokes equation, with significant savings in the computer time required for the numerical simulations.

The nonlinear heat transfer with phase change in the composite structures consisting of the PCM-impregnated metal matrix is governed by the Fourier equation

$$\frac{\partial(\rho c T)}{\partial t} = \nabla \cdot (k \nabla T) \tag{1}$$

where T is the temperature, t is the time, ρ, c, and k are the density, specific heat capacity, and thermal conductivity, respectively. The apparent heat capacity method was used to account for the latent heat of phase change because it allows a more accurate description of the enthalpy-temperature relation compared to the standard enthalpy-porosity method implemented in ANSYS Fluent, which always assumes a linear variation of enthalpy with temperature. According to the apparent heat capacity method, in the parts of the computational domain corresponding to the PCM an apparent specific heat $c = c_{app} = \partial h_{\mathrm{PCM}}/\partial T$ is assumed, where h_{PCM} is the enthalpy per unit mass of the PCM [14,18]

$$h_{PCM} = \int_{T_{ref}}^{T} \left[c_{PCM} + L_{PCM} \frac{\partial \beta}{\partial T} \right] \mathrm{d}T \tag{2}$$

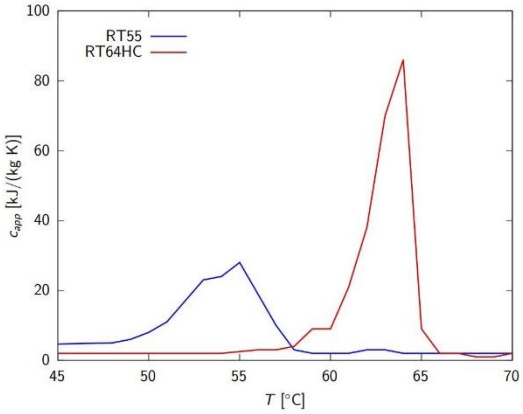

Figure 2. Temperature dependence of the apparent specific heat of the considered paraffins [15].

In the previous equation, c_{PCM} and L_{PCM} are the specific heat capacity and latent heat of phase change of the PCM, respectively, β is the liquid fraction during the melting process and T_{ref} is the reference temperature. The temperature dependence of the apparent specific c_{app} of the paraffins considered here is show in figure 2.

The spatial periodicity of the 20 mm thick metal structures together with the boundary conditions which only include one heated external surface, while all the other ones are adiabatic, allowed the use of reduced computational domains corresponding to repetitive geometries that, because of the existing symmetries, could be further reduced to the parts highlighted in orange shown in figure 3(a,b) for the BCC5 and BCC10 structures. In the same figure, the corresponding computational grids are also shown together with the boundary conditions (figure 3(c,d)). Those grids were chosen based on grid independence tests that proved that the results were nearly mesh independent when the grid size was equal or smaller than 0.2 mm in the PCM and 0.1 mm in the metal for the BCC5 structure and 0.25 mm and 0.2 mm for the BCC10. The adopted grids consisted of 435 012 and 341 152 tetrahedral cells for BCC5 and BCC10, respectively.

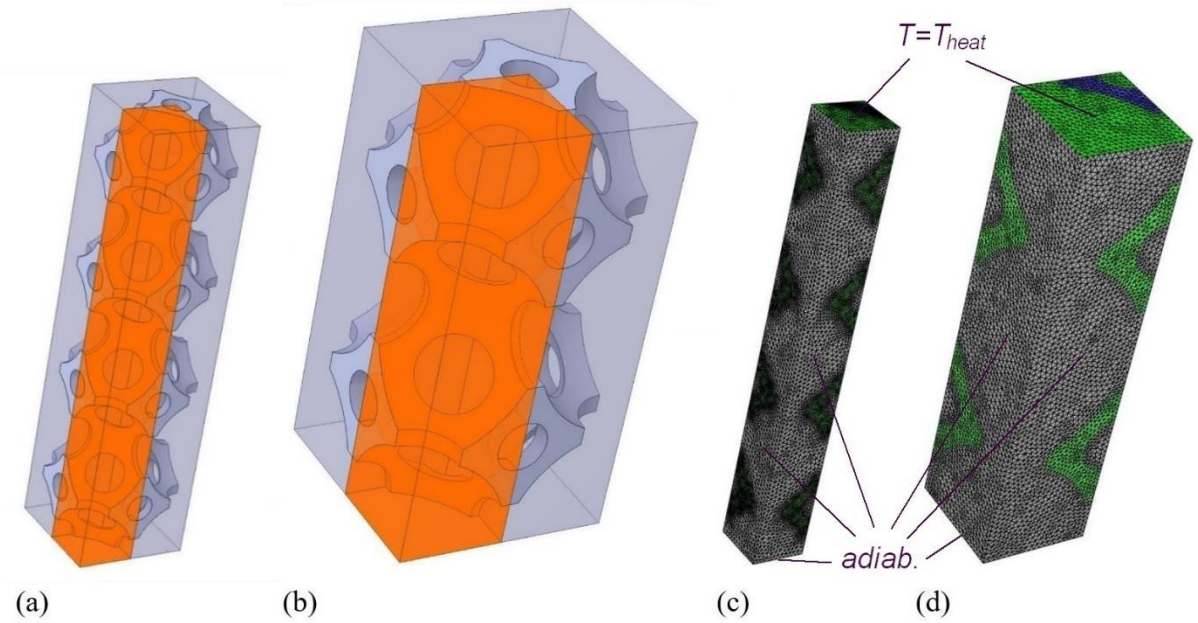

Figure 3. Computational domains (in orange): (a) BCC5 and (b) BCC10; computational grids and boundary conditions: (c) BCC5 and (d) BCC10.

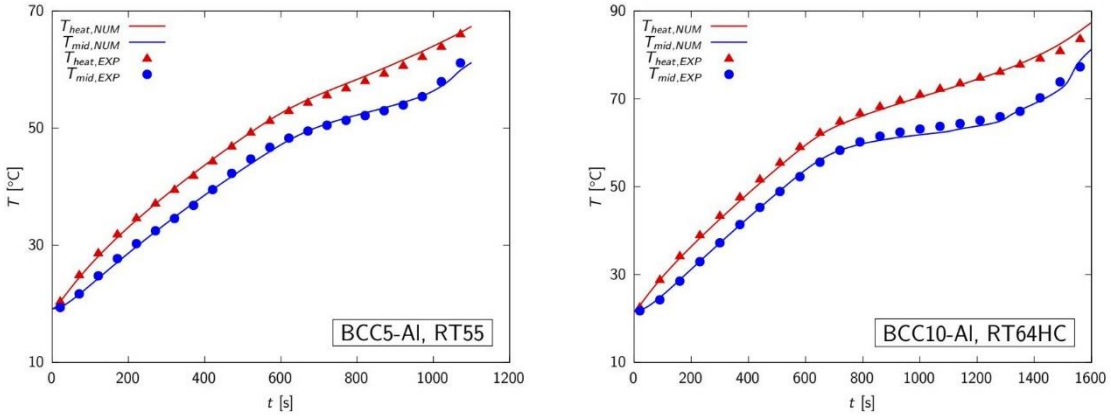

Figure 4. Comparisons of numerical (solid curves) and experimental (symbols) temperature-time histories for different structures and PCMs and an applied heat flux equal to 10 kW m^{-2} [14].

Time integration was performed using an implicit second order method. Up to 25 iterations were required within each time step, with an absolute tolerance on the residuals set at 10^{-9}. Time step independence tests showed that time steps between 4 s and 8 s, depending on the cell size and the paraffin wax, were adequate to yield accurate transient numerical simulations.

The adopted numerical model had been previously validated through comparison with experimental data obtained with reference to the same metal matrices and PCMs considered here, that however were part of test modules with a size of 100×100 mm^2 that also included two 10 mm thick metal plates, a heater, and an insulating structure [14]. The tests were carried out for three values of the heat flux on the heated surface, namely, 10, 15, and 20 kW m^{-2}. The comparisons concerned the temperature-time profiles on the heated surface (T_{heat}) and on the midplane (T_{mid}) of the test modules as shown in the examples reported in figure 4 for the combinations BCC5-Al and RT55, and BCC10-Al and RT64HC, when the heat flux applied on the heated surface is 10 kW m^{-2}. In all cases, the average discrepancies between numerical and experimental values are around 1 K with reference to both T_{heat} and T_{mid}. As can be seen, the agreement between experimental and computed results is very good and is comparable to that obtained for the other values of the applied heat flux, not reported here for brevity [14]. All this confirms the validity of the adopted simplified numerical model, which can then be confidently used to carry out systematic studies aimed at assessing the performance of cellular structures like the ones considered in this work.

4. Numerical results and discussion

The experimentally validated numerical model was used to investigate the thermal performance of the four cellular structures described in Section 2 (BCC5-Al, BCC5-Cu, BCC10-Al and BCC10-Cu) impregnated with the two paraffins, in temperature intervals of 10 K that include their respective melting ranges. The specified initial and heated surface temperatures were 49°C and 59°C in the test cases involving the RT55 wax and 57°C and 67°C in those involving the RT64HC.

To give some physical insight into the phase change process in PCM-impregnated metal matrices, a time series of temperature maps on the surfaces of the computational domains are shown as in figure 5 for the BCC5-Cu and BCC10-Cu structures and the RT64HC paraffin. It is apparent that in both cases the melting of the PCM starts near the metal ligaments, but then it proceeds much faster in the BCC5 case because the finer metal matrix allows a more effective heat penetration into the low thermal conductivity phase change material. In this example, at t = 720 s the melting of the PCM is almost complete in the BCC5-Cu structure, while it is still far behind in the BCC10-Cu case.

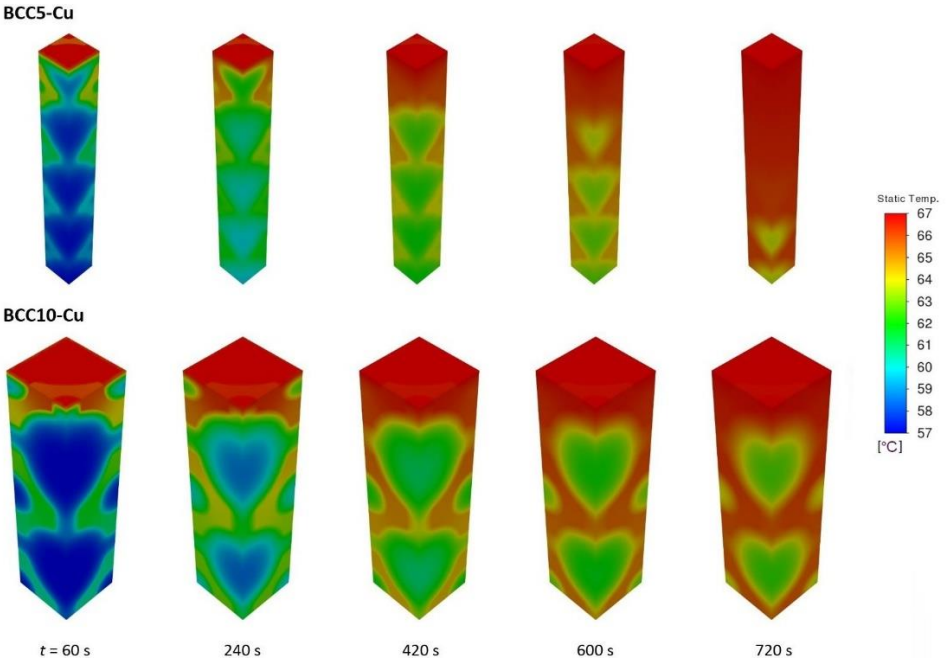

Figure 5. Temperature color maps at different times for the BCC5-Cu and BCC10-Cu structures and the RT64HC paraffin.

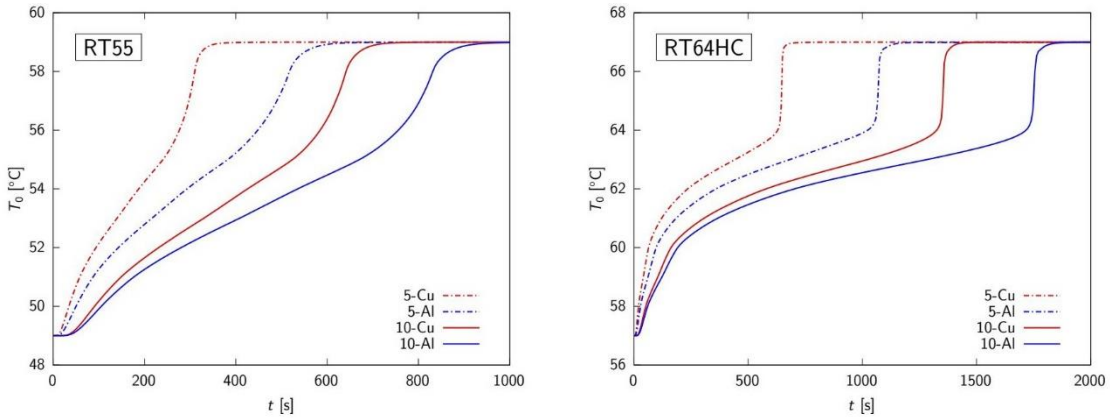

Figure 6. Time profiles of the temperature T_0 in the coldest point of the adiabatic surface.

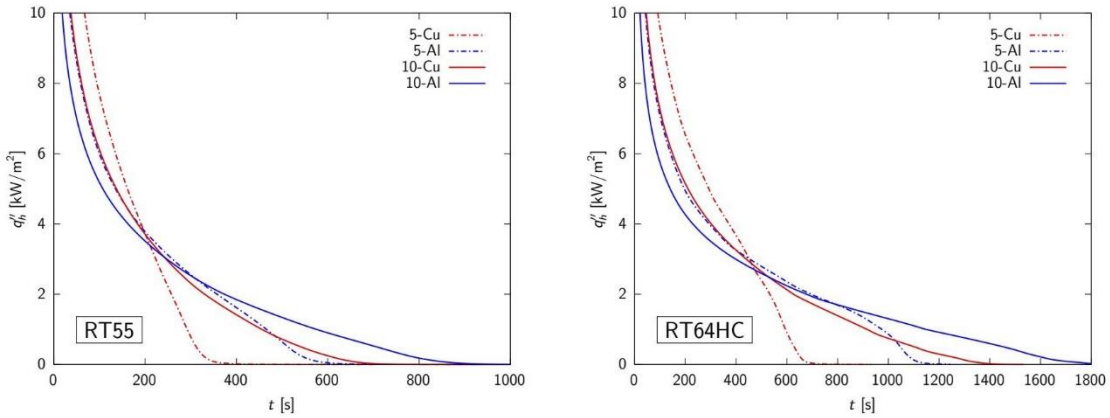

Figure 7. Time histories of the of the instantaneous heat fluxes q_h'' through the heated surfaces.

More quantitative results are reported in Figure 6, which shows the time profiles of the temperature T_0 in the coldest point of the adiabatic surface opposite to the heated one for all the composite structures considered. This kind of plots allow an accurate estimation of the time for complete melting in different conditions and, in the present case, clearly demonstrate that with the BCC5-Cu structure the melting process is significantly faster than with all the other structures. As already observed, this can be ascribed to the finer cellular structure of the BCC5, but also to the higher thermal conductivity of the copper solid matrix.

The time histories of the of the instantaneous heat fluxes q_h'' through the heated surfaces are shown in figure 7. The values of q_h'' are very large at the beginning of the transients, with the slope of the curves pertaining to the BCC5-Cu being the highest. Then the heat fluxes decrease gradually to approach zero when all the PCM is melted. For each structure, the trends of the curves obtained with the two paraffins are similar, but, obviously, the durations of the transients are different because of the larger latent heat of phase change of the RT64HC paraffin compared to that of the RT55.

The trends in time of the stored thermal energy H per unit area of the heated surface can be obtained as the time integral of the corresponding values of the heat flux q_h'' and are shown in Figure 8. The values of the energy density $E_d = H_{max}/s$, where H_{max} is the maximum value of H and s is the thickness of the structure, together with those of the periods of time τ in which the systems actually transfers energy and of the average power densities $q_{ave} = E_d/\tau$ during the thermal energy storage processes are reported in table 3 for all the cases considered. As can be seen, the maximum energy stored in each composite structure mainly depends on the properties of the paraffin waxes, since the heat capacity of the metal matrices only have a marginal effect. However, the rates of energy accumulation are very different for the four BCC structures considered, with the BCC5-Cu yielding the best performance for the reasons outlined above. This aspect is of primary interest for practical applications, particularly in cases where a PCM-impregnated structure is used for the thermal management of devices operating intermittently.

Table 3. Energy and power densities.

Paraffin	**RT55**				**RT64HC**				**Units**
BCC	**5-Al**	**5-Cu**	**10-Al**	**10-Cu**	**5-Al**	**5-Cu**	**10-Al**	**10-Cu**	
E_d	107.7	108.9	107.8	109.2	188.2	189.5	188.3	189.7	[kJ m^{-3}]
τ	543	317	801	606	1052	627	1620	1239	[s]
q_{ave}	198.5	343.5	134.6	180.3	179.0	302.4	116.3	153.2	[W m^{-3}]

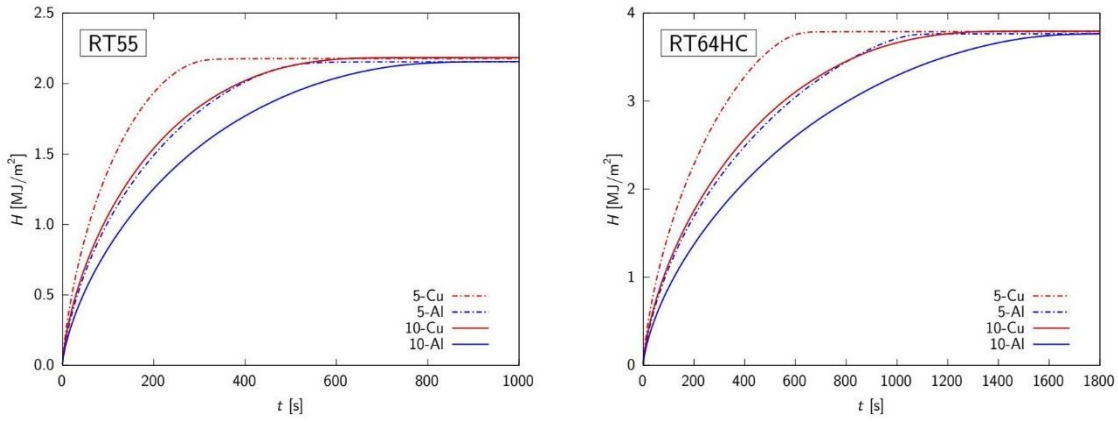

Figure 8. Trend in time of the stored thermal energy H per unit area of the heated surface.

5. Conclusions

A numerical investigation was conducted concerning the thermal performance of composite structures consisting of a PCM-impregnated cellular metal matrix, which can be obtained by additive manufacturing technologies. The purpose of the metal matrix is to increase the effective thermal conductivity of the phase-change material to enable the speed-up of the thermal energy storage and release processes. Possible applications concern the thermal control of electronic components, particularly those that operate intermittently.

Two body-centered cubic (BCC) structures with cell sizes of 5 and 10 mm and a porosity of 87%, two metal matrix materials, namely, an aluminum alloy and copper, and two paraffins were considered. Numerical simulations were conducted using the commercial code ANSYS Fluent and a purely conductive heat transfer model since previous experimental results had shown that, with the structures considered in this work, the effects of natural convection in the molten PCM are negligible. Thermal transients were analyzed and PCM melting times were compared under the assumption that the temperature of one of the surfaces of the solid PCM-impregnated structure was instantaneously raised to a value higher than that of complete melting of the phase-change material.

The results of the comparisons, which concerned the PCM melting times, the instantaneous heat fluxes at the heated surfaces and the time trends of the thermal energy stored in the structure, showed that the best thermal performance is achievable with smaller cell sizes because they allow a more effective heat penetration into the PCM. In addition, thermal performances are also significantly affected by the thermal conductivities of solid materials, even when these are very high as in the present case. Future work includes the analysis of the thermal behavior of other composite structures in an optimization perspective.

Acknowledgements

The supports of the MIUR through the PRIN Project 2017F7KZWS is gratefully acknowledged.

References

[1] Maranda S, Sponagle B, Worlitschek J and Groulx D 2019 *Appl. Sci.* **9** 4613
[2] Baby B and Balaji C 2014 *Int. J. Therm. Sci.* **79** 240–249
[3] Baby B and Balaji C 2013 *Appl. Therm. Eng.* **54** 65–77
[4] Singh A, Rangarajan S, Choobineh L and Sammakia B 2021 *IEEE Trans. Compon. Packaging Manuf. Technol.* **11** 1783–1791
[5] Krishnan S, Garimella SV and Kang SS 2005 *IEEE Trans. Compon. Packaging Technol.* **28** 281–289
[6] Yang H, Li Y, Zhang L, Zhu Y 20021 *Int. J. Heat Mass Transf.* **181** 121899
[7] Sahoo SK, Das MK, Rath P 2016 *Renewable Sustainable Energy Rev.* **59** 550–582
[8] Zhu Z-Q, Huang Y-K, Hu N, Zeng Y, Fan L-W 2018 *Appl. Therm. Eng.* **128** 966-972
[9] Yang H, Li Y, Yang Y, Chen D, Zhu Y 2020 *Int. J. Heat Mass Transf.* **147** 118974
[10] Khodadadi JM, Fan L, Babaei H 2013 *Renewable Sustainable Energy Rev.* **24** 418–444
[11] Righetti G, Savio G, Meneghello R, Doretti L and Mancin S 2020 *Int. J. Therm. Sci.* **153**, 106376
[12] Diani A, Moro L and Rossetto L 2021 *Appl. Sci.* **11** 5396
[13] Moon H, Miljovic N and King WP 2020 *Int. J. Heat Mass Transf.* **153** 119591
[14] Diani A, Nonino C and Rossetto L 2022 *Appl. Therm. Eng.* **215** 118969
[15] Rubitherm Technologies GmBH Available online: https://www.rubitherm.eu/en/index.php/productcategory/organische-pcm-rt
[16] Lafdi K, Mesalhy O and Shaikh S 2007 *J. Appl. Phys.* **102** 083549
[17] ANSYS, Inc., ANSYS Fluent Theory Guide, Release 17.0 (2016).
[18] Tamma KK and Namburu RR 1990 *Int. J. Numer. Methods Eng.* **30** 803–820.